

Shape recognition and classification in electro-sensing

Habib Ammari^a, Thomas Boulier^a, Josselin Garnier^{b,1}, and Han Wang^a

^aDepartment of Mathematics and Applications, Ecole Normale Supérieure, 75005 Paris, France; and ^bLaboratoire de Probabilités et Modèles Aléatoires and Laboratoire Jacques-Louis Lions, Université Paris Diderot, 75205 Paris Cedex 13, France

Edited* by George Papanicolaou, Stanford University, Stanford, CA, and approved June 20, 2014 (received for review April 9, 2014)

This paper aims at advancing the field of electro-sensing. It exhibits physical mechanisms underlying shape perception for weakly electric fish. These fish orient themselves at night in complete darkness by using their active electrolocation system. They generate a stable, relatively high-frequency, weak electric field and perceive the transdermal potential modulations caused by a nearby target with different electromagnetic properties than the surrounding water. The main result of this paper is a scheme that explains how weakly electric fish might identify and classify a target, knowing in advance that the latter belongs to a certain collection of shapes. The scheme is designed to recognize living biological organisms. It exploits the frequency dependence of the electromagnetic properties of living organisms, which comes from the capacitive effects generated by the cell membrane structure. When measurements are taken at multiple frequencies, the fish might use the spectral content of the perceived transdermal potential modulations to classify the living target.

inverse conductivity problem | polarization tensor | shape classification

In the turbid rivers of Africa and South America, some species of fish generate a stable, relatively high-frequency (0.1–10 kHz), weakly electric (≤ 100 mV/cm) field that is not enough for defense against predators. In 1958, Lissmann and Machin (1) discovered that the emitted electrical signal is in fact used for active electro-sensing. The weakly electric fish have thousands of receptors at the surface of their skins. A nearby target with different admittivity than the surrounding water perturbs the transdermal potential induced by the electric organ discharge (2, 3). Targets with large permittivity cause appreciable phase shifts, which can be measured by receptors called T-type units (4). It is an important input for the fish, and thus it will be the central point in this paper for shape classification.

Active electro-sensing has driven an increasing number of experimental, behavioral, biological, and computational studies since Lissmann and Machin's work (5–12). Behavioral experiments have shown that weakly electric fish are able to locate a target (12) and discriminate between targets with different shapes (13) or/and electric parameters (conductivity and permittivity) (14). The growing interest in electro-sensing could be explained not only by the curiosity of discovering a sixth sense, electric perception, that is not accessible by our own senses, but also by potential bio-inspired applications in underwater robotics. It is challenging to equip robots with electric perception and provide them, by mimicking weakly electric fish, with imaging and classification capabilities in dark or turbid environments (14–20).

Mathematically speaking, the problem is to locate the target and identify its shape and material parameters given the current distribution over the skin. Due to the fundamental ill-posedness of this imaging problem, it is very intriguing to see how much information weakly electric fish are able to recover. The electric field perturbation due to the target is a complicated highly nonlinear function of its shape, admittivity, and distance from the fish. Thus, understanding analytically this electric sensing is likely to give us insight in this regard (5–7, 9, 13, 18, 21). Although locating targets from the electric field perturbations induced on the skin of the fish is now understood (17, 22), identifying and classifying their shapes are considered to be some of the most challenging problems in electro-sensing. Although

the neuroethology of these fish has been significantly advanced recently (see ref. 23 and references therein), the neural mechanisms encoding the shape of a target are far beyond the scope of our study. Rather, this work focuses on the physical feasibility of such a process, which was not explained before.

In ref. 22, a rigorous model for the electro-location of a target around the fish was derived. Using the fact that the electric current produced by the electric organ is time harmonic with a known fundamental frequency, a space-frequency location search algorithm was introduced. Its robustness with respect to measurement noise and its sensitivity with respect to the number of frequencies, the number of sensors, and the distance to the target were illustrated. In the case of disk- and ellipse-shaped targets, the conductivity, the permittivity, and the size of the targets can be reconstructed separately from multifrequency measurements. Such measurements have been used successfully in transadmittance scanners of breast tumors (24–26).

The main result of this paper is the presentation and analysis of a scheme that allows to recognize and classify targets from multifrequency measurements of the electric field perturbations induced by the targets. To explain how the shape information is encoded in measured data, we distinguish two cases: recognition of nonbiological targets and recognition of living organisms. Most of the nonbiological objects have very low permittivities, and therefore, their electromagnetic parameters are frequency independent. Living targets have frequency-dependent electromagnetic parameters because their cell membrane structures induce capacitive effects (27), and therefore it is possible to exploit the spectral content of the data. We will mostly focus our attention on the second situation, but we first explain the strategy for the first one. Our model in this paper of the weakly electric fish relies on differential imaging, i.e., by forming an image from the perturbations of the field due to the target. The method is based on the multipole expansion for the perturbations of the electric field induced by a nearby target in terms of the characteristic size of the target. The asymptotic expansion derived in refs. 22 and 28 generalizes Rasnow's equation (29) in two directions: (i) it is a higher-order approximation of the effect of a nearby target, and it is valid for an arbitrary shape and admittivity contrast; and (ii) it also takes into account the body of the fish. As was first shown in ref. 22, one can reduce the

Significance

Weakly electric fish orient themselves in complete darkness by using their active electrolocation system. They generate a weak electric field and perceive the transdermal potential modulations caused by a nearby target with different electromagnetic properties than the surrounding water. The main result of this paper is a scheme that explains how weakly electric fish might identify and classify living biological organisms. This scheme exploits the frequency dependence of the electromagnetic properties of living organisms, which comes from the capacitive effects generated by the cell membrane structure.

Author contributions: H.A., T.B., J.G., and H.W. designed research, performed research, and wrote the paper.

The authors declare no conflict of interest.

*This Direct Submission article had a prearranged editor.

¹To whom correspondence should be addressed. Email: garnier@math.univ-paris-diderot.fr.

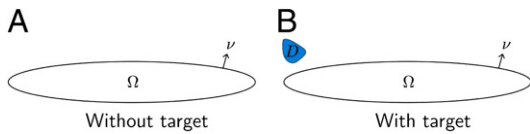


Fig. 1. Geometric setup without (A) and with (B) a target. The ellipse is the fish body Ω . The blue domain in B is the target D .

multipole formula to the one in free space, i.e., without the fish. In this paper we show how to identify and classify a target, knowing in advance that the latter belongs to a dictionary of precomputed shapes. The shapes considered in this paper have been experimentally tested, and the results are reported in ref. 30. This idea comes naturally in mind when modeling behavioral experiments such as in refs. 12–14. The precomputed shapes would then be a model for the memory of the fish (trained to recognize specific shapes), and the experience of recognition discussed here would simulate the discrimination exercises that are then carried out by them. We developed two algorithms for shape classification: the first one is based on shape descriptors for nonbiological targets and the second one is based on spectral-induced polarizations that can be used to image living biological targets. In the first one, we first extract, from the data, generalized (or high-order) polarization tensors of the target (GPTs) (28). These tensors, first introduced in ref. 31, are intrinsic geometric quantities and constitute the right class of features to represent the target shapes (32, 33). The shape features are encoded in the polarization tensors. The extraction of the GPTs can be achieved by a least-squares method. The noise level in the reconstructed GPTs depends on the angle of view. The larger the angle of view, the more stable the reconstruction. Then we compute from the extracted features invariants under rigid motions and scaling. Comparing these invariants with those in a dictionary of precomputed shapes, we can successfully classify the nonbiological target. For living biological targets, because the measurements are taken at multiple frequencies, we make use of the spectral content of the data to improve considerably the stability with respect to measurement noise of the physics-based classification procedure. In fact, we show that the first-order polarization tensors at multiple frequencies are sufficient for the purpose of classification of living biological targets. This result is described in detail in the following sections.

Feature Extraction from Induced Current Measurements

Electro-Sensing Model. Let us recall the model of electro-sensing: the body of the fish is Ω , an open bounded set in \mathbb{R}^d , $d = 2, 3$ with smooth boundary, and with outward normal unit vector denoted by ν (Fig. 1A). The electric organ is a time-harmonic dipole $f(x) \exp(i\omega t)$ inside Ω or a sum of point sources inside Ω satisfying the charge neutrality condition, where ω is the operating frequency. The skin of the fish is very thin and highly resistive. Its effective

thickness, that is, the skin thickness times the contrast between the water and the skin conductivities, is denoted by ξ , and it is of the order of 1/10th of the fish size (5). We assume that the permittivity ε_0 of the background medium is vanishing, and we denote by σ_0 its conductivity. We consider a target $D = z + B$, where z is its location, and B is a smooth bounded domain containing the origin (Fig. 1B). We assume that D is of complex admittivity $k = \sigma + i\varepsilon\omega$, with ω being the operating frequency and σ and ε being, respectively, the conductivity and the permittivity of the target.

It has been shown in ref. 22 that, in the presence of D , the electric potential generated by the fish is of the form $u(x) \exp(i\omega t)$ where u is the solution of the following equations:

$$\begin{aligned} \nabla \cdot \sigma_0 \nabla u &= f \quad \text{in } \Omega \\ \nabla \cdot [\sigma_0 + (k - \sigma_0)\chi_D] \nabla u &= 0 \quad \text{in } \mathbb{R}^d \setminus \bar{\Omega}, \end{aligned}$$

together with the boundary conditions

$$\frac{\partial u}{\partial \nu} \Big|_- = 0, \quad u|_+ - u|_- = \xi \frac{\partial u}{\partial \nu} \Big|_+ \quad \text{on } \partial\Omega,$$

and the behavior at infinity

$$|u(x)| = O(|x|^{-d+1}), \quad |x| \rightarrow \infty.$$

Here, χ_D is the characteristic function of D , $\partial/\partial\nu$ is the normal derivative, and $|_{\pm}$ denotes the limits from, respectively, outside and inside Ω . Fig. 2 shows isopotentials with and without a target with zero permittivity but different conductivity from the surrounding medium. In this figure, $\varepsilon = 0$ so that the potential is a real field that does not depend on the operating frequency. In the same configuration, Fig. 3 shows contour lines of the potential perturbation, which is the difference of the potentials obtained with and without the target plotted in Fig. 2 B and A, respectively. One can clearly see that the potential within the fish is not affected by the target. Indeed the potential inside the body of the fish Ω is the solution to the interior problem with Neumann boundary conditions at $\partial\Omega$, and therefore it does not depend on the target. The potential outside the body is affected by the target, and the target seems to play the role of a dipole for the potential perturbation (Fig. 3). This observation will be clarified in the forthcoming asymptotic analysis. In practice, the receptors at the surface of the skin of the fish perceive the transdermal potential, that is, the jump of the potential $u|_+ - u|_-$. Because the potential at the interior of the body of the fish is not affected by the target, the perturbation of the transdermal potential is equal to the potential perturbation at the exterior surface of the skin. In the following, we will study the latter. It is also worth emphasizing that if the admittivity k of the target depends

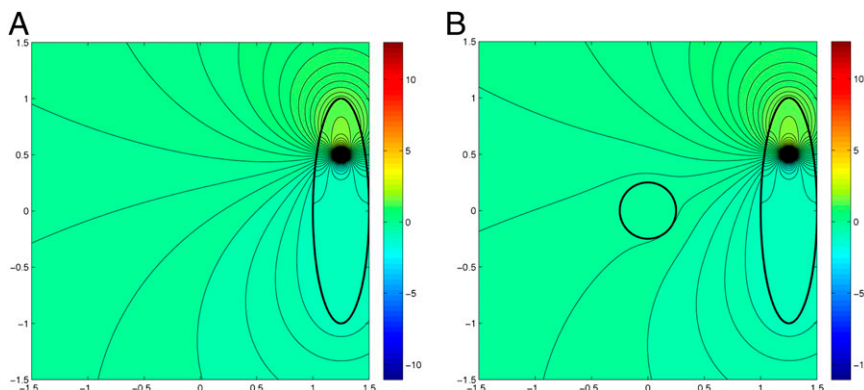


Fig. 2. The isopotentials without (A) and with (B) a target. The ellipse is the fish body Ω . The disk in B is the target D . The source is a dipole inside Ω . Here, $\sigma_0 = 1$, $\sigma = 5$, $\varepsilon = 0$, and $\xi = 0.1$.

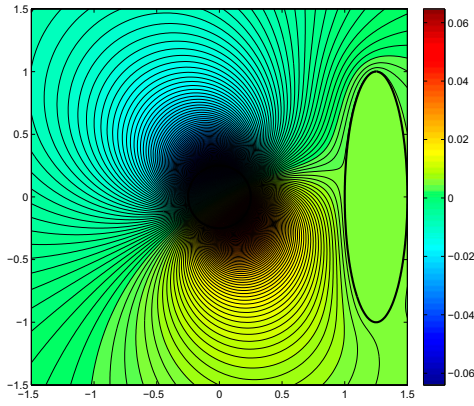


Fig. 3. The contour lines of the potential perturbation, that is, the difference between the potentials with and without of the target. It is the same configuration as in Fig. 2. The potential perturbation is zero inside the fish. The potential perturbation at the exterior surface of the fish is not zero and contains information about the target.

on the frequency (i.e., if the permittivity ε is nonzero), then a phase shift in the potential is induced, that is, u is complex-valued and depends on the frequency.

Asymptotic Formalism. The first step is to compute the polarization tensors from the measurements. In this regard, the next asymptotic result will be useful. Except when mentioned, we will fix in this section the frequency ω , leading to a fixed complex admittivity k . Let $G(x)$ be the Green function of the Laplacian in \mathbb{R}^d , which satisfies $\Delta G = \delta$ (where δ is the Dirac function at the origin) and is given by

$$G(x) = \begin{cases} \frac{1}{2\pi} \ln|x|, & d=2 \\ -\frac{1}{4\pi} \frac{1}{|x|}, & d=3. \end{cases}$$

We denote the single and double layer potentials of a function $\phi \in L^2(\partial\Omega)$ as $S_\Omega[\phi]$ and $D_\Omega[\phi]$, where

$$S_\Omega[\phi](x) := \int_{\partial\Omega} G(x-y)\phi(y)d\sigma(y), \quad x \in \mathbb{R}^d, \quad [1]$$

and

$$D_\Omega[\phi](x) := \int_{\partial\Omega} \frac{\partial G}{\partial \nu(y)}(x-y)\phi(y)d\sigma(y), \quad x \in \mathbb{R}^d \setminus \partial\Omega. \quad [2]$$

We also define the Neumann-Poincaré operator \mathcal{K}_Ω^* by

$$\mathcal{K}_\Omega^*[\phi](x) := \int_{\partial\Omega} \frac{\partial G}{\partial \nu(x)}(x-y)\phi(y)d\sigma(y), \quad x \in \partial\Omega, \quad [3]$$

for $\phi \in L^2(\partial\Omega)$. We assume that the target is away from the fish, i.e., the distance between the fish and the target is much larger than the characteristic size of the target but smaller than the range of the electrolocation, which does not exceed two fish body lengths. The following dipole expansion for the potential at the exterior surface of the skin of the fish holds when the volume of the target becomes small.

Proposition 1. Let the source f be a dipole of moment $p_0 \in \mathbb{R}^d$ placed at z_0 . Let the function $H: \mathbb{R}^d \rightarrow \mathbb{C}$ be defined by

$$H(x) = \frac{1}{\sigma_0} p_0 \cdot \nabla G(x-z_0) + (S_\Omega - \xi D_\Omega) \left[\frac{\partial u}{\partial \nu} \Big|_+ \right] (x). \quad [4]$$

Then the following approximation holds

$$u(x) = H(x) - \sum_{\alpha, \beta=1}^d \partial_{z_\alpha} H(z) M_{\alpha\beta}(\lambda, B) \partial_{z_\beta} G(z-x), \quad [5]$$

uniformly for $x \in \partial\Omega$, where z is the location of the target D and

$$M_{\alpha\beta}(\lambda, B) := \int_{\partial B} (\lambda \mathcal{I} - \mathcal{K}_B^*)^{-1} [\nu_\alpha](y) y_\beta d\sigma(y),$$

is the first-order polarization tensor (PT) associated with domain B and the contrast $\lambda = (k + \sigma_0)/[2(k - \sigma_0)]$ (33). Here, \mathcal{K}_B^* is the Neumann-Poincaré operator associated with B and \mathcal{I} is the identity operator.

Let us make a few remarks. First, the definition of the PT still holds for complex-valued λ . However, some properties are lost by this change; thus, one has to study them more carefully in this situation. Second, the function H , which is computed from the boundary measurements, still depends on the target, but this is not important for our present study. Indeed, Eq. 5 could have been derived with U , the background solution in the absence of the target, instead of H and G_R —the Green function associated to Robin conditions on $\partial\Omega$ —instead of G , but it is much easier to compute $\partial_{z_\alpha} H(z)$ and $\partial_{z_\beta} G(z-x)$ once z is known. This discussion leads us to the third remark: the location z is supposed to be known from the algorithm developed in ref. 22. Electrolocation algorithms are based on a space-frequency approach in the case of multifrequency measurements (or on the fish movement if only one frequency is used) (17, 22). The fourth remark follows from the scaling relation

$$M_{\alpha\beta}(\lambda, \delta B) = \delta^d M_{\alpha\beta}(\lambda, B),$$

which shows that, in the context of a small volume $\delta \ll 1$, the first-order correction in Eq. 5 is of the order of δ^d , whereas the rest is of order δ^{d+1} .

Data Acquisition. Let us suppose that the fish is moving, and let us take a sample of $S \in \mathbb{N}^*$ different positions $(\Omega_s)_{1 \leq s \leq S}$. For a fixed frequency, this gives us $2S$ different functions, $(u_s)_{1 \leq s \leq S}$ and $(H_s)_{1 \leq s \leq S}$, leading us to the following data matrix:

$$\begin{aligned} \mathbb{Q} &:= (Q_{sr})_{1 \leq s \leq S, 1 \leq r \leq R}, \\ Q_{sr} &:= H_s(x_r^{(s)}) - u_s(x_r^{(s)}), \quad 1 \leq s \leq S, \quad 1 \leq r \leq R, \end{aligned} \quad [6]$$

where $(x_r^{(s)} \in \partial\Omega_s)_{1 \leq r \leq R}$ are the receptors of the fish being in the s th position. The choices of indices are motivated by the fact that

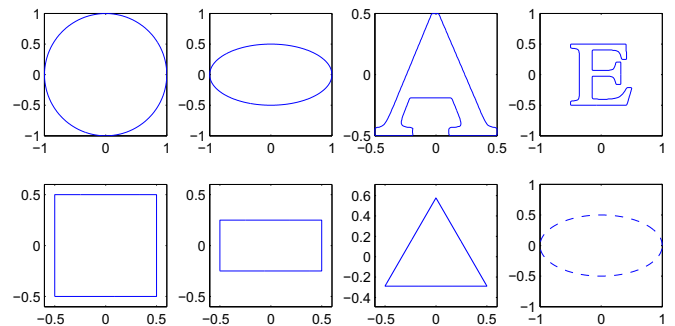


Fig. 4. The eight elements of the dictionary. The first seven element have parameters $\sigma = 2$ and $\varepsilon = 1$. The eighth element (with dashed lines) indicates a target with different electrical parameters $\sigma = 5$ and $\varepsilon = 2$.

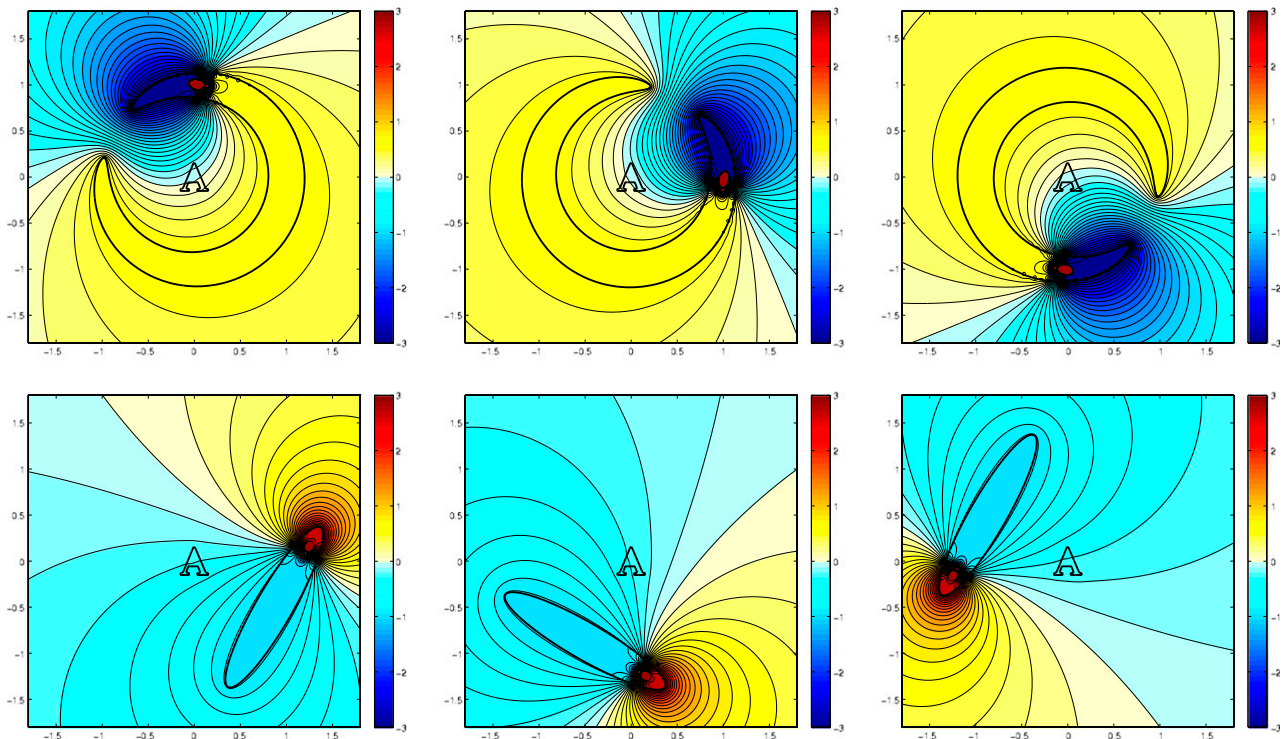


Fig. 5. Two different kinds of experiences involve (Upper) a twisted-ellipse shape or (Lower) a straight ellipse shape. The real part of the electric field is plotted for 3 of 20 positions that the fish takes around the target (placed at the origin).

the different positions play the role of sources. From Eq. 5, one has

$$Q_{sr} = \sum_{\alpha, \beta=1}^d \partial_{z_\alpha} H_s(z) M_{\alpha\beta}(\lambda, B) \partial_{z_\beta} G(z - x_r^{(s)}), \quad [7]$$

up to a small error, and we can therefore extract the PT $\mathbb{M}(\lambda, B) := [M_{\alpha\beta}(\lambda, B)]_{\alpha, \beta=1}^d$ by a standard least-squares procedure (28).

In the case of multifrequency measurements $(\omega_1, \dots, \omega_F)$, we can reconstruct $(\mathbb{M}^{(f)})_{1 \leq f \leq F}$ from $(Q^{(f)})_{1 \leq f \leq F}$ analogously.

It is worth mentioning that the location of the target detected by the fish may be different from the true one due to error in the electrolocation procedure. Moreover, the target may be rotated, and hence, the reconstructed PTs correspond to a translated, scaled, and rotated target B . To recognize the shape B , it is therefore fundamental for the recognition procedure to have size invariance, rotational invariance, and translational invariance. The schemes that we introduce below have these desirable properties, which makes them robust with respect to the electrolocation procedure in particular.

Recognition and Classification

We focus on the first-order polarization tensors in the case $d = 2$, that is, the 2×2 complex matrix $\mathbb{M}^{(f)}(D)$ associated with the target D and frequency ω_f

$$M_{\alpha\beta}^{(f)}(D) := \int_{\partial D} \left[\frac{\sigma + \sigma_0 + i\omega_f \varepsilon}{2(\sigma - \sigma_0 + i\omega_f \varepsilon)} \mathcal{I} - \mathcal{K}_D^* \right]^{-1} [\nu_\alpha](y) y_\beta d\sigma(y),$$

for $f = 1, \dots, F$, $\alpha, \beta = 1, 2$. We will show that they are sufficient to identify efficiently the targets provided that their electrical permittivity is not small at low frequencies. Such an imaging approach exploits the capacitive effect induced by cell membranes and is called capacitive imaging.

We use the spectral dependence of the first-order PTs for recognition. We have the following properties (33).

Proposition 2. For any scaling parameter $\delta > 0$, rotation angle $\theta \in \mathbb{R}$, and translation vector $z \in \mathbb{R}^2$, let us denote

$$D = z + \delta \mathbb{R}_\theta B := \{z + \delta \mathbb{R}_\theta u, \quad u \in B\},$$

where

$$\mathbb{R}_\theta := \begin{pmatrix} \cos \theta & -\sin \theta \\ \sin \theta & \cos \theta \end{pmatrix},$$

is the rotation matrix of angle θ . Then

$$\mathbb{M}^{(f)}(D) = \delta^2 \mathbb{R}_\theta \mathbb{M}^{(f)}(B) \mathbb{R}_\theta^T. \quad [8]$$

Hence, if we denote by $\tau_1^{(f)}(D)$ and $\tau_2^{(f)}(D)$ the singular values of $\mathbb{M}^{(f)}(D)$, we obtain $\tau_j^{(f)}(D) = \delta^2 \tau_j^{(f)}(B)$, $j = 1, 2$.

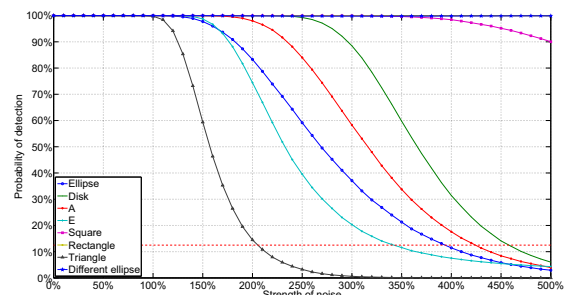


Fig. 6. Stability of classification based on differences between all singular values of PTs, when the fish is a twisted ellipse. The characteristic size of the target is supposed to be known.

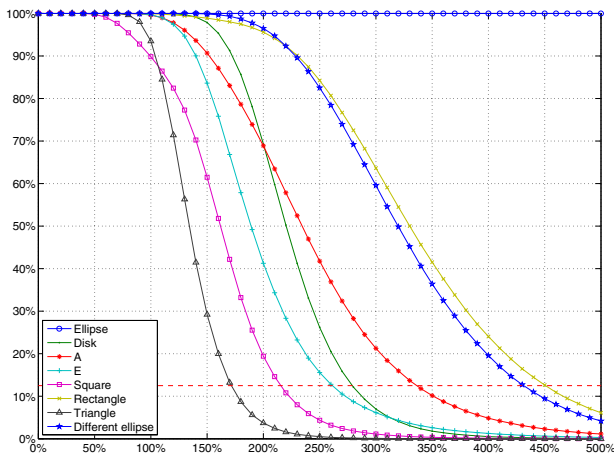


Fig. 7. Same as in Fig. 6 when the fish is a straight ellipse.

This proposition gives an idea for two algorithms:

- i) The first one, matching the singular values of all the first-order PTs $(\mathbb{M}^{(f)})_{1 \leq f \leq F}$, would be dependent of the characteristic scale δ of the targets in the dictionary; and
- ii) The second one, independent of the scale of the target, would match the following quantities:

$$\mu_j^{(f)} = \frac{\tau_j^{(f)}}{\tau_j^{(F)}} \quad \text{for } j=1, 2 \quad \text{and } f=1, \dots, F-1. \quad [9]$$

Some comments are in order. First, the reason why we consider the first one, even if it is scale dependent, is because it is far more stable. Also, in some biological experiments, two targets of different scales are considered as different (13). A question raised was “how is it possible to discriminate between a nearby small target and an extended one situated far away?” With the second algorithm, we have an answer. The last remark concerns Eq. 9. We could have also considered other scale-independent ratios, such as

$$\frac{\tau_j^{(f)}}{\tau_j^{(1)}} \quad \text{or} \quad \frac{\tau_j^{(f)}}{\sum_{f=1}^F \tau_j^{(f)'}}$$

but because $\tau_j^{(F)}$ happens to be the largest one (the frequencies are sorted in increasing order), it is more stable to consider Eq. 9. It is worth mentioning that if there exists an integer $p > 2$ such that $\mathbb{R}_{2\pi/p} D = D$, then $\mathbb{M}^{(f)}(D)$ is isotropic.

Numerical Illustrations

In this section, we illustrate the performance of the algorithms developed in the previous section. When, at multiple frequencies, the first-order polarization tensors are used, we arrive at a very robust and efficient classification procedure from spectral data.

Setup and Methods. We describe the dictionary and the measurement systems. We consider two different shapes for the fish: ellipses and twisted ellipses. This variety of shapes exists in nature. On the one hand, twisted ellipses would represent electric eels (*Electrophorus electricus*), whereas on the other hand, straight ellipses would look like *Apteronotids* (3). This simplified representation shows that the principle of our algorithms can be generalized to any kind of fish shape (hence, modeling, for example, electro-sensing for *Mormyrids* as well). It also enhances the fact that, for bio-inspired engineering applications, the shape of the robot is not a determining factor. Moreover, as we will see later, our simplified representation is a good model to tackle aperture issues.

Dictionary. The dictionary \mathcal{D} that we consider is composed by eight different targets: a disk, an ellipse, the letter A, the letter E, a rectangle, a square, a triangle, and an ellipse with different electrical parameters (Fig. 4). Indeed, the first seven targets have conductivity $\sigma = 2$ and permittivity $\varepsilon = 1$, whereas the last one has conductivity $\sigma = 5$ and permittivity $\varepsilon = 2$.

Measurements. In each numerical experiment, one target of the dictionary is placed at the origin while the fish swims around it. We consider two different shapes for the body of the fish: straight ellipses and twisted ellipses. The measured data are built taking 20 positions of the fish around the target (Fig. 5).

The typical size of the target is $\delta = 0.3$ (which means, the target is one of the elements of the dictionary shown in Fig. 4 scaled by δ). The fish is turning around a disk of radius $R = 1$ and center at 0; the semiaxes of the twisted ellipse are $a = 1.8$ and $b = 0.2$, whereas the ones of the straight ellipse are $a = 1$ and $b = 0.2$. The effective thickness of the skin is set at $\xi = 0$. The fish has 64 receptors uniformly distributed on its skin, and the electric organ emits $F = 10$ frequencies, equally distributed from $\omega_0 := 1$ to $F\omega_0$. We refer to ref. 22 for nondimensionalization of the underlying model equations with proper quantities and realistic values.

Classification. The recognition process is as follows. When measurements are acquired, we perform least-square reconstruction of the PTs of the targets. From these PTs, we compute quantities of interest q (i.e., singular values or ratios of singular values). Then, for each element B_n in the dictionary \mathcal{D} , we compute $\|q - q(B_n)\|$, where $q(B_n)$ is the precomputed quantity of interest for the n th shape, and we decide that the target is of type \hat{n} that achieves the minimum of $\|q - q(B_n)\|$.

Framework for algorithms of multifrequency classification:

- i) Input: the quantities of interest $(q^{(f)})_{1 \leq f \leq F}$ calculated from the measurement of an unknown shape D ;
- ii) For $B_n \in \mathcal{D}$ do;
- iii) $e_n \leftarrow \sum_{1 \leq f \leq F} \|q(B_n)^{(f)} - q^{(f)}\|^2$, where $[q(B_n)^{(f)}]_{1 \leq f \leq F}$ is the same type of quantity of interest of shape B_n ;
- iv) $n \leftarrow n + 1$;
- v) End for
- vi) Output: the estimated dictionary element $\hat{n} \leftarrow \operatorname{argmin}_n e_n$.

Stability Analysis. First, let us explain what kind of noise is considered. We will add a random matrix (with Gaussian entries) to the data matrix \mathbb{Q} defined in Eq. 6. More precisely, we will consider $\tilde{\mathbb{Q}} := \mathbb{Q} + \varepsilon_n \mathbb{W}$, where \mathbb{W} is a $S \times R$ matrix whose coefficients follow a complex Gaussian distribution with mean 0 and variance 1. The real number ε_n is the strength of the noise and will be given in percentage of the fluctuations of \mathbb{Q} (i.e., $\max_{s,r} Q_{sr} - \min_{s,r} Q_{sr}$). The recognition procedure remains the same. Stability analysis was then carried out empirically: for each noise level, we performed $N_{\text{exp}} = 5 \times 10^4$ independent recognition processes and computed the ratio of good detection. The computation ends when we reach

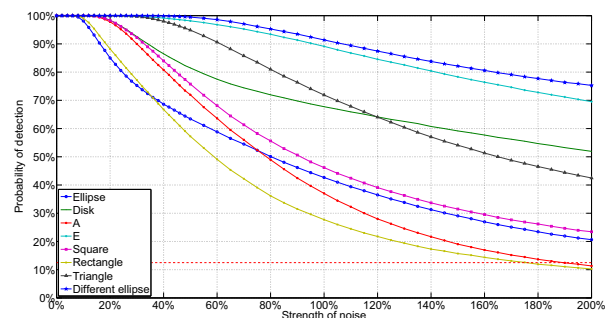


Fig. 8. Stability of classification based on differences between ratios of singular values, when the fish is a twisted ellipse.

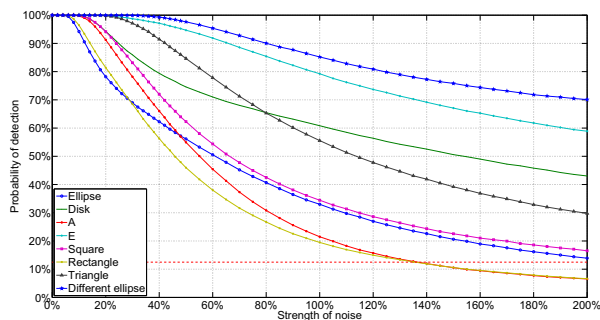


Fig. 9. Same as in Fig. 8 when the fish is a straight ellipse.

the threshold of 12.5% probability of detection that corresponds to a uniform random choice of the object in the dictionary. The numerical results are plotted in Figs. 6–9.

Results and Discussion. One can see that considering all singular values (Figs. 6 and 7) is much more stable than considering ratios of singular values (Figs. 8 and 9). Moreover, the aperture does not change the stability very much. In this regard, the most stable algorithm is to recognize all singular values when the fish is a twisted ellipse (Fig. 6), leading us to a probability of detection superior to 90% with noise level of 125%. The noise level is computed with respect to the perturbation in the measurements \mathcal{Q} given by Eq. 6, which is of the order of the target volume as seen in Eqs. 7 and 8. Hence, a noise level of 125% remains small compared with the actual transdermal potential u .

Concluding Remarks

In this paper, we successfully exhibited some fundamental physical mechanisms for possible shape recognition and classification in active electrolocation. When measurements at multiple frequencies are used, the classification exploits the measured

frequency-dependent first-order polarization tensors. The resulting classification scheme is very robust with respect to additive noise. However, it can only be used for imaging living biological organisms, for which the permittivity is not zero.

In the case of nonbiological targets with very low electrical permittivity, such as man-made conducting or insulating structures, the data are frequency independent. It is then necessary to introduce another scheme for classifying nonbiological targets. A possible classification scheme is based on the measured generalized (or high-order) polarization tensors of the target. The electric fish could extract, from the measured perturbations of the transdermal potential, such geometric features, and it could compute, from the extracted features, invariants under rigid motions and scaling that can be considered as shape descriptors. The weakly electric fish might then classify a target by comparing its invariants with those of a set of learned shapes. We showed in ref. 28 that extracting generalized polarization tensors from the frequency-independent data and comparing invariants with those of learned elements in a dictionary yields a classification procedure with a good performance in the full-view case and with small measurement noise level. However, this shape descriptor-based classification is quite unstable in the limited-view case and for high noise level.

In conclusion, the recognition and classification procedure that we provide in this paper is much more stable and easy to implement for imaging living biological organisms than for imaging nonbiological targets with very low permittivity, for which the proposed multifrequency approach cannot be applied.

The principle of our algorithms can be generalized to any kind of fish shape. For bio-inspired engineering applications, the shape of the autonomous robot is not determining. The results of this paper could motivate the equipment of autonomous robots with electro-sensing capabilities to image, recognize, and classify both living organisms and nonbiological targets.

ACKNOWLEDGMENTS. This work was supported by European Research Council Advanced Grant Project MULTIMOD–267184.

- Lissmann HW, Machin KE (1958) The mechanism of object location in gymnochirus niloticus and similar fish. *J Exp Biol* 35(2):451–486.
- Bastian J (1981) Electrolocation i. how the electroreceptors of apteronotus albifrons code for moving objects and other electrical stimuli. *J Comp Physiol A Neuroethol Sens Neural Behav Physiol* 144(4):465–479.
- Moller P (1995) *Electric Fish: History and Behavior* (Chapman and Hall, London).
- Nelson ME (2005) *Target Detection, Image Analysis, and Modeling* (Springer-Verlag, New York).
- Assad C (1997) Electric field maps and boundary element simulations of electrolocation in weakly electric fish. PhD thesis (California Institute of Technology, Pasadena, CA).
- Babineau D, Longtin A, Lewis JE (2006) Modeling the electric field of weakly electric fish. *J Exp Biol* 209(Pt 18):3636–3651.
- Budelli R, Caputi AA (2000) The electric image in weakly electric fish: Perception of objects of complex impedance. *J Exp Biol* 203(Pt 3):481–492.
- Chen L, House JL, Krahe R, Nelson ME (2005) Modeling signal and background components of electroreceptive scenes. *J Comp Physiol A Neuroethol Sens Neural Behav Physiol* 191(4):331–345.
- Maciver MA (2001) The computational neuroethology of weakly electric fish: Body modeling, motion analysis, and sensory signal estimation. PhD thesis (University of Illinois at Urbana-Champaign, Champaign, IL).
- Maciver MA, Sharabash NM, Nelson ME (2001) Prey-capture behavior in gymnotid electric fish: Motion analysis and effects of water conductivity. *J Exp Biol* 204(3):543–557.
- Rasnow B, Assad C, Nelson ME, Bower JM (1989) Simulation and measurement of the electric fields generated by weakly electric fish. *Advances in Neural Information Processing Systems 1*, ed Touretzky DS (Morgan Kaufmann Publishers, San Mateo, CA), pp 436–443.
- Von der Emde G, Schwarz S, Gomez L, Budelli R, Grant K (1993) Electric fish measure distance in the dark. *Science* 260:1617–1623.
- Von der Emde G, Fetz S (2007) Distance, shape and more: Recognition of object features during active electrolocation in a weakly electric fish. *J Exp Biol* 210(Pt 17):3082–3095.
- Von der Emde G (1999) Active electrolocation of objects in weakly electric fish. *J Exp Biol* 202(Pt 10):1205–1215.
- Curet OM, Patankar NA, Lauder GV, Maciver MA (2011) Aquatic manoeuvring with counter-propagating waves: A novel locomotive strategy. *J R Soc Interface* 8(60):1041–1050.
- Jawad B, et al. (2010) Sensor model for the navigation of underwater vehicles by the electric sense. *Proceedings of the 2010 IEEE International Conference on Robotics and Biomimetics* (IEEE Conference Proceedings, Piscataway, NJ), pp 879–884.
- Lebastard V, et al. (2010) Underwater robot navigation around a sphere using electrolocation sense and Kalman filter. *Proceedings of the 2010 IEEE/RSJ International Conference on Intelligent Robots and Systems* (IEEE Conference Proceedings, Piscataway, NJ), pp 4225–4230.
- Porez M, Lebastard V, Ijspeert AJ, Boyer F (2011) Multi-physics model of an electric fish-like robot: Numerical aspects and application to obstacle avoidance. *Proceedings of the 2011 IEEE/RSJ International Conference on Intelligent Robots and Systems* (IEEE Conference Proceedings, Piscataway, NJ), pp 1901–1906.
- Postlethwaite CM, Psemeneke TM, Selimkhanov J, Silber M, MacIver MA (2009) Optimal movement in the prey strikes of weakly electric fish: A case study of the interplay of body plan and movement capability. *J R Soc Interface* 6(34):417–433.
- Solberg JR, Lynch KM, MacIver MA (2008) Active electrolocation for underwater target localization. *Int J Robot Res* 27(5):529–548.
- Boyer F, Gossiaux P-B, Jawad B, Lebastard V, Porez M (2012) Model for a sensor inspired by electric fish. *IEEE Trans Robot* 52(2):492–505.
- Ammari H, Boulier T, Garnier J (2013) Modeling active electrolocation in weakly electric fish. *SIAM J. Imag. Sci.* 6(1):258–321.
- Bullock TH, Hopkins CD, Popper AN, Richard RF, eds (2005) *Electroreception* (Springer-Verlag, New York).
- Ammari H, Kwon O, Seo JK, Woo EJ (2004) T-scan electrical impedance imaging system for anomaly detection. *SIAM J Appl Math* 65:252–266.
- Kim S, Lee J, Seo JK, Woo EJ, Zribi H (2008) Multifrequency trans-admittance scanner: mathematical framework and feasibility. *SIAM J Appl Math* 69:22–36.
- Scholz B (2002) Towards virtual electrical breast biopsy: Space-frequency MUSIC for trans-admittance data. *IEEE Trans Med Imaging* 21(6):588–595.
- Miklavcic D, Paveselj N, Hart FX (2006) *Electric Properties of Tissues* (Wiley Encyclopedia of Biomedical Engineering, Hoboken, NJ).
- Ammari H, et al. (2014) Target identification using dictionary matching of generalized polarization tensors. *Found Comput Math* 14:27–62.
- Rasnow B (1996) The effects of simple objects on the electric field of apteronotus. *J Comp Physiol A Neuroethol Sens Neural Behav Physiol* 178:397–411.
- Von der Emde G (2004) Distance and shape: Perception of the 3-dimensional world by weakly electric fish. *J Physiol Paris* 98(1-3):67–80.
- Ammari H, Kang H (2003) High-order terms in the asymptotic expansions of the steady-state voltage potentials in the presence of conductivity inhomogeneities of small diameter. *SIAM J Math Anal* 34(5):1152–1166.
- Ammari H, Garnier J, Kang H, Lim M, Yu S (2014) Generalized polarization tensors for shape description. *Numer Math* 26:199–224.
- Ammari H, Kang H (2007) Polarization and moment tensors. *Applied Mathematical Sciences*, Vol 2 (Springer, New York).